

ORIGINAL ARTICLE

Open Access



Quantitative comparison of data-driven gating and external hardware gating for ^{18}F -FDG PET-MRI in patients with esophageal tumors

Sofia Kvernby^{1,2*} , Nafsika Korsavidou Hult^{1,3}, Elin Lindström^{1,2}, Jonathan Sigfridsson³, Gustav Linder⁴, Jakob Hedberg⁴, Håkan Ahlström^{1,3,5}, Tomas Bjerner^{1,3} and Mark Lubberink^{1,2}

* Correspondence: sofia.kvernby@akademiska.se

¹Radiology & Nuclear Medicine, Department of Surgical Sciences, Uppsala University, Uppsala, Sweden

²Medical Physics, Uppsala University Hospital, Entrance 85, SE-751 85 Uppsala, Sweden

Full list of author information is available at the end of the article

Abstract

Background: Respiratory motion during PET imaging reduces image quality. Data-driven gating (DDG) based on principal component analysis (PCA) can be used to identify respiratory signals. The use of DDG, without need for external devices, would greatly increase the feasibility of using respiratory gating in a routine clinical setting. The objective of this study was to evaluate data-driven gating in relation to external hardware gating and regular static image acquisition on PET-MRI data with respect to SUV_{max} and lesion volumes.

Methods: Sixteen patients with esophageal or gastroesophageal cancer (Siewert I and II) underwent a 6-min PET scan on a Signa PET-MRI system (GE Healthcare) 1.5–2 h after injection of 4 MBq/kg ^{18}F -FDG. External hardware gating was done using a respiratory bellow device, and DDG was performed using MotionFree (GE Healthcare). The DDG raw data files and the external hardware-gating raw files were created on a Matlab-based toolbox from the whole 6-min scan LIST-file. For comparison, two 3-min static raw files were created for each patient. Images were reconstructed using TF-OSEM with resolution recovery with 2 iterations, 28 subsets, and 3-mm post filter. SUV_{max} and lesion volume were measured in all visible lesions, and noise level was measured in the liver. Paired *t*-test, linear regression, Pearson correlation, and Bland-Altman analysis were used to investigate difference, correlation, and agreement between the methods.

Results: A total number of 30 lesions were included in the study. No significant differences between DDG and external hardware-gating SUV_{max} or lesion volumes were found, but the noise level was significantly reduced in the DDG images. Both DDG and external hardware gating demonstrated significantly higher SUV_{max} (9.4% for DDG, 10.3% for external hardware gating) and smaller lesion volume (– 5.4% for DDG, – 6.6% for external gating) in comparison with non-gated static images.

(Continued on next page)

(Continued from previous page)

Conclusions: Data-driven gating with MotionFree for PET-MRI performed similar to external device gating for esophageal lesions with respect to SUV_{max} and lesion volume. Both gating methods significantly increased the SUV_{max} and reduced the lesion volume in comparison with non-gated static acquisition. DDG resulted in reduced image noise compared to external device gating and static images.

Keywords: Respiratory gating, DDG, PET-MRI, Esophageal tumors

Background

Respiratory motion during PET imaging of anatomical structures in the thorax and upper abdomen reduces image quality, resulting in decreased lesion detection and quantitative accuracy by introducing an underestimation of the standardized uptake value (SUV) and an overestimation of the lesion volume (Liu et al. 2009). Correction for respiratory motion in PET images can be performed in various ways. External hardware gating is based on tracking breathing motion externally, either by visually recording the movement of the chest wall or by using an external bellow device and then splitting the breathing cycle into different phases. Image reconstruction can then be performed by only using data from static gates of the breathing cycle, usually during exhale position (quiescent phase gating). To avoid decreased signal-to-noise ratio (SNR) due to reduction in count statistics, this method requires prolonged acquisition times.

For PET/MRI scanners, different MRI techniques can be used to detect motion. For example, analysis of shifts and rotations in k-space data can be used to estimate motion (Grimm et al. 2015), MRI image tagging can be used to detect deformation of tissue (Guérin et al. 2011), and very fast imaging sequences and navigator techniques can be used for tracing respiratory motion during PET-acquisition (Würslein et al. 2013), but in that case at the expense of reduced time to acquire clinically relevant MRI sequences and putting constraints on the PET/MRI imaging protocol.

Principal component analysis (PCA), which is a mathematical technique investigating changes in a dataset, can be used to extract respiratory motion patterns from raw PET list-mode data. Data-driven gating (DDG) based on PCA can be used to identify respiratory signals, similarly as external hardware gating does, and sort data into respiratory phases containing no, or very little, respiratory motion. DDG was first introduced by Thielemans et al. in 2011 (Thielemans et al. 2011) and has demonstrated promising results in several studies on PET-CT systems (Büther et al. 2016; Walker et al. 2019), showing high agreement with external device gating. On PET/MRI systems, device-less DDG has been used in combination with a short additional dynamic MRI scan for correction of breathing motion with good results (Manber et al. 2015).

Recently, GE Healthcare released a version of DDG based on PCA for PET-MRI scanners, as part of a research agreement, implemented in a Matlab-based Toolbox (Duetto, GE Healthcare, Waukesha). The use of DDG, without need for external devices, would greatly increase the feasibility of using respiratory gating in a routine clinical setting. The objective of this study is to evaluate DDG in relation to external hardware gating and regular static image acquisition on PET-MRI data in patients with esophageal cancer.

Methods

Sixteen patients with esophageal and gastroesophageal junctional (GEJ) tumors were included in the study. Patient characteristics are described in detail in another study (Linder et al. 2019); in brief, inclusion criteria were potentially resectable tumors (T_{1-4a} , N_{1-3} , M_0) and histologically verified esophageal or GEJ cancer (Siewert I and II). The patients were asked for study participation in the clinical setting after cancer diagnosis. PET-MRI was performed in conjunction with the routine PET-CT investigation to conclude clinical staging. All patients provided written informed consent to participate in the study, and approval was granted from the regional medical ethics committee in Uppsala (DNR 2014/551).

Image acquisition and reconstruction

All patients underwent a 6-min PET scan on a 3T Signa PET-MRI system (GE Healthcare) 109 ± 21 min after injection of 4 MBq/kg ^{18}F -FDG. The PET system has an axial and transaxial field of view (FOV) of 25 cm and 60 cm, respectively, producing 89 image planes with a slice thickness of 2.8 mm. Data were acquired in list mode to enable reconstruction of data in different time frames and breathing gates retrospectively.

External hardware gating was performed using an MRI-compatible respiratory bellow device, and a quiescent phase-based gating method (Q.Static, GE Healthcare) was used for the whole 6-min scan. Static gates were automatically extracted during end-expiration of the breathing cycle to form a gating phase free from motion (Soussan et al. 2016). The external gating triggers were stored in the PET list file, which enables retrospective unlisting of gated data during the quiescent phase. The quiescent phase includes 50% of the total breathing cycle, resulting in maintained PET coincidence data equivalent to a 3-min static scan.

The DDG was performed using MotionFree (GE Healthcare), which uses PCA to derive the respiratory waveforms directly from the PET coincidence data. In short, data are binned into 0.5-s sinograms, and the frequency of the motion can be determined by using the Fourier transform. Respiratory motion is defined as motion originating from frequencies in the range of 0.1–0.4 Hz, implying a respiratory cycle of 2.5–10 s. To establish the impact of the motion on the data, an R value is calculated as the ratio between the peak value within this respiratory frequency range and the mean value above the respiratory frequency range.

The whole 6-min PET list file was transferred to a Matlab-based toolbox containing the DDG MotionFree package (Duetto v02.03, GE Healthcare). In the toolbox, respiratory waveforms are derived from the PET-coincidence data, and DDG respiratory gating triggers are stored in the PET list file in the same way as for the external gating triggers. For the data-driven gating, an R value was given for each patient, describing the impact of respiratory motion on the data, where a threshold of $R=15$ is the default value recommendation for MotionFree.

Raw files were created in the toolbox by unlisting the static gates from the whole 6-min scan list file. For comparison with the gated data and for investigation of normal image quality variation in a scan-rescan situation, two 3-min static raw files (0–3 min and 3–6 min) were also created for each patient.

All images were reconstructed using TF-OSEM with resolution recovery, 2 iterations, 28 subsets, and a 3-mm Gaussian post-processing filter. A 60-cm FOV was used with a 192×192 reconstruction matrix, resulting in a $3.125 \times 3.125 \times 2.80$ mm³ voxel size.

Image analysis

SUV images were calculated by dividing the activity concentrations with the amount of injected activity per body weight. Images were visually assessed with respect to image artifacts and reconstruction errors. Esophageal lesions and lymph nodes were identified on the PET images, and SUV_{max} as well as lesion volume, based on a 41% SUV_{max} threshold (Boellaard et al. 2015), were measured using Hermes Affinity Viewer 1.1 (Hermes Medical Solutions). For image noise measurement, a spherical volume of interest with a diameter of 3 cm was placed in the liver in all images, and SUV mean values together with standard deviations were measured. Noise level was defined as the standard deviation divided by the mean SUV. To estimate the effect of lesion position on the efficacy of DDG, the vertical distance from the center of the lesion to the top of the liver was measured. Lesions below 1 cm³ were represented separately in graphs.

Statistics

Results are presented as mean \pm standard deviation unless otherwise specified. Data representing SUV_{max} and lesion volume were not normally distributed, while data representing changes in these parameters were normally distributed according to Shapiro-Wilk normality tests. To determine whether SUV_{max} and lesion volume measured in images with either of the two respiratory motion correction methods, external hardware gating and DDG, differed from those of a static non motion-corrected image, a non-parametric paired Wilcoxon test was used. Correlation between both gating methods and non-gated images was assessed using linear regression and Spearman correlation coefficients for SUV_{max} and lesion volume. To investigate agreement between DDG and external hardware gating, Bland-Altman analysis was performed for SUV_{max} and lesion volume values. Correlation between the distance from the lesion to the diaphragm, and the increase in SUV_{max} respectively the decrease in lesion volume, were assessed using Pearson correlation coefficients. Similarly, the correlation between the DDG R value, and the increase in SUV_{max} respectively the decrease in lesion volume, were assessed using Pearson correlation coefficients.

Results

Sixteen PET-MRI examinations and a total number of 30 lesions (up to four lesions and lymph nodes per subject) were included in the study. The average R value given by DDG was 17.9 (range 6.9–28.7). In 75% of the patients, the DDG analysis estimated an R value greater than 15, implying a significant impact from breathing motion. Hence, only patients with an R value > 15 were included in the further analysis, in total 12 patients and 23 lesions.

In DDG images, the average lesion volume and SUV_{max} were 6.3 ± 9.1 cm³ (mean \pm SD; range 0.14–32.0 cm³) and 30.8 ± 27.4 g/ml (range 8.8–130.6 g/ml). For external device-gated images, the average lesion volume and SUV_{max} were 6.2 ± 9.0 cm³ (mean \pm SD; range 0.19–31.2 cm³) and 31.0 ± 28.4 g/ml (range 9.3–134.8 g/ml).

No significant differences ($p > 0.05$) were found between the data-driven gating and the external hardware-gating SUV_{max} or lesion volumes; a good correlation ($R^2 = 0.987$ for SUV_{max} and $R^2 = 0.985$ for lesion volume) between the methods could be seen. A Bland-Altman analysis was performed to compare and visually illustrate data from the

two gating methods, which demonstrated a small non-significant bias (0.7% for SUV_{max} and -3.7% for lesion volume) with 95% limits of agreement of -16.2 to 17.7% for SUV_{max} and -46.7 to 39.3% for lesion volume (Figs. 1 and 2). Excluding lesions $< 1\text{cm}^3$, as indicated by the open symbols in Figs. 1 and 2, showed even higher agreement between DDG and external gating (bias -0.5% for SUV_{max} and 0.2% for lesion volume; the 95% limits of agreement were -15.1 to 14.1% for SUV_{max} and -0.9 to 1.2% for lesion volume).

In static non-gated images, the average lesion volume and SUV_{max} were $6.3 \pm 9.2\text{ cm}^3$ (mean \pm SD; range 0.2–31.3 cm^3) and $30.7 \pm 23.8\text{ g/ml}$ (range 10.3–119.5 g/ml) for the first 3 min of acquisition and $6.7 \pm 9.2\text{ cm}^3$ (range 0.3–31.4 cm^3) and $28.1 \pm 22.8\text{ g/ml}$ (range 6.9–112.8 g/ml) for the last 3 min of acquisition.

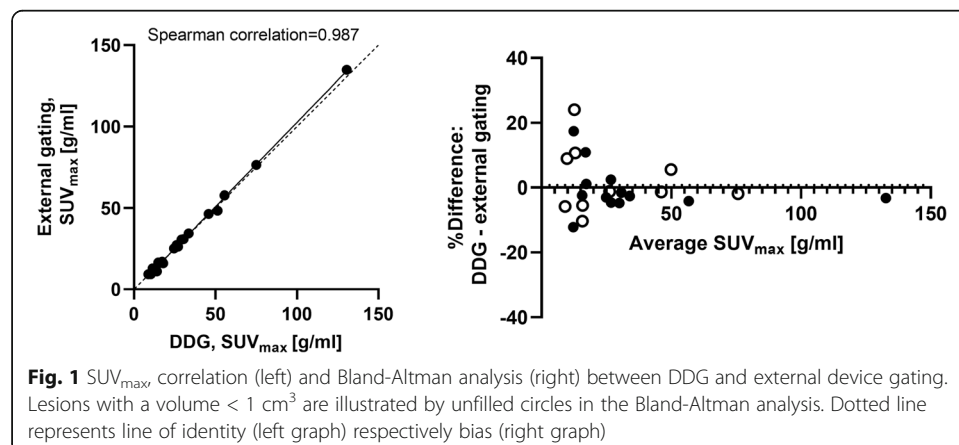
Both external device gating and DDG significantly influenced SUV_{max} and lesion volumes compared with the static non-gated images. The average SUV_{max} increased significantly ($p < 0.05$) compared with the static acquisition based on data from the last 3 min of acquisition, for both DDG (9.4% increase, from 28.1 to 30.8) and the external hardware-gating method (10.3% increase, from 28.1 to 31.0). Furthermore, the average lesion volume decreased significantly ($p < 0.05$) for both DDG (-5.4% decrease, from 6.7 to 6.3 cm^3) and external device gating (-6.6% from 6.7 to 6.2 cm^3). When instead comparing the gated data with the first 3 min of static acquisition, similar improvement in SUV_{max} and lesion volumes could be found, but this was not significant ($p > 0.05$). Results are illustrated in Fig. 3.

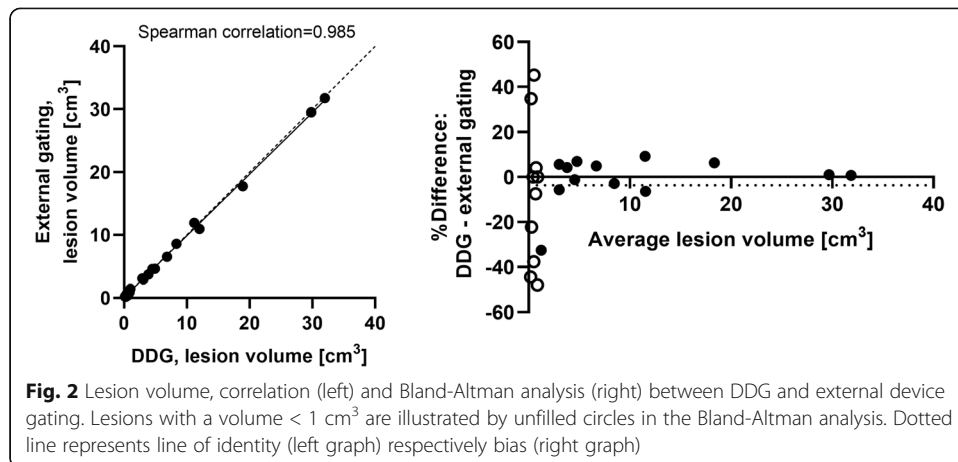
Evaluating the correlation between the lesion's distance to the diaphragm and the improvement in image accuracy (increase in SUV_{max} or decrease in lesion volume), the results did not demonstrate any clear correlation between respiratory gating methods and a static acquisition (Fig. 5). Similarly, the results did not demonstrate any strong correlation between R value and increase in SUV_{max} or decrease in lesion volume (Fig. 6).

Quantitative measures of noise level in the liver are presented in Table 1. The results demonstrated that the noise level in images based on data-driven gating, 0.165, was significantly lower ($p < 0.001$) than in images based on either external hardware gating (noise level 0.235) or regular static acquisition (noise level 0.223 and 0.225).

Discussion

In this study, we evaluated data-driven gating with MotionFree against external hardware gating and static acquisition. We found that data-driven gating performs





equivalent to external hardware gating for esophageal lesions in a PET-MRI scanner with respect to lesion volume and SUV_{max} . Our findings are in accordance with the results from recently published studies using DDG performed on PET-CT systems (Walker et al. 2018; Büther et al. 2020; Bertolli et al. 2018).

Both data-driven gating and external hardware gating retained ~50% of the coincidence data from a 6-min scan and significantly increased SUV_{max} and decreased lesion volume compared with a static 3-min acquisition that maintained all coincidence data.

No difference in SUV_{max} or lesion volumes was found between images based on data-driven gating and images based on external device gating, but we found that the

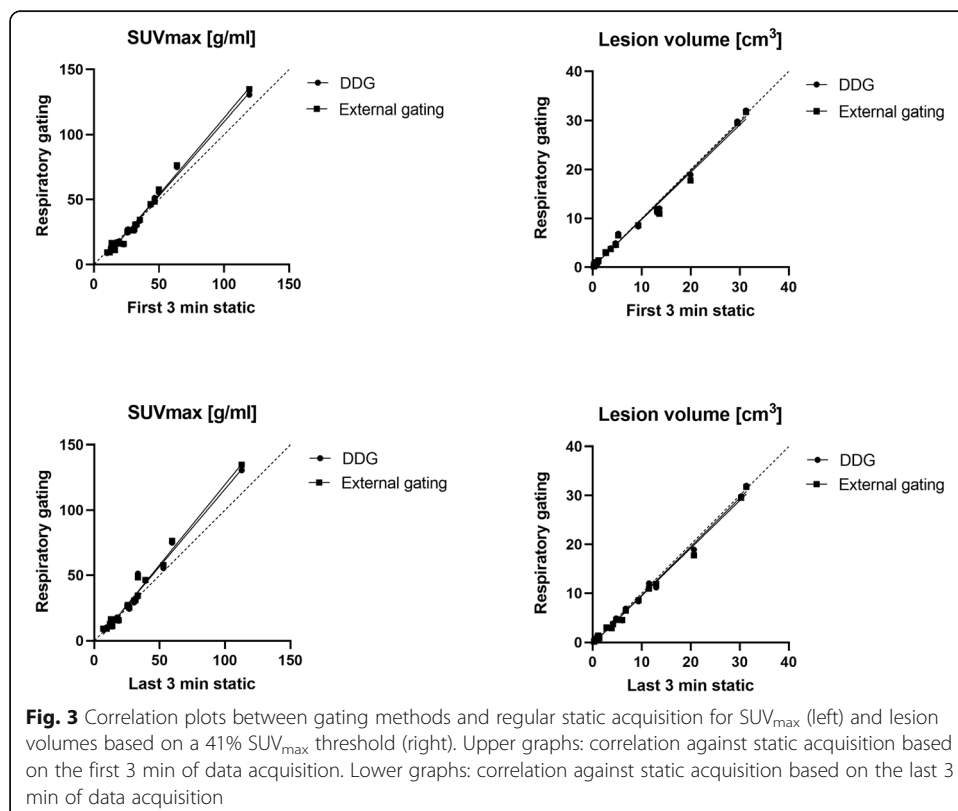
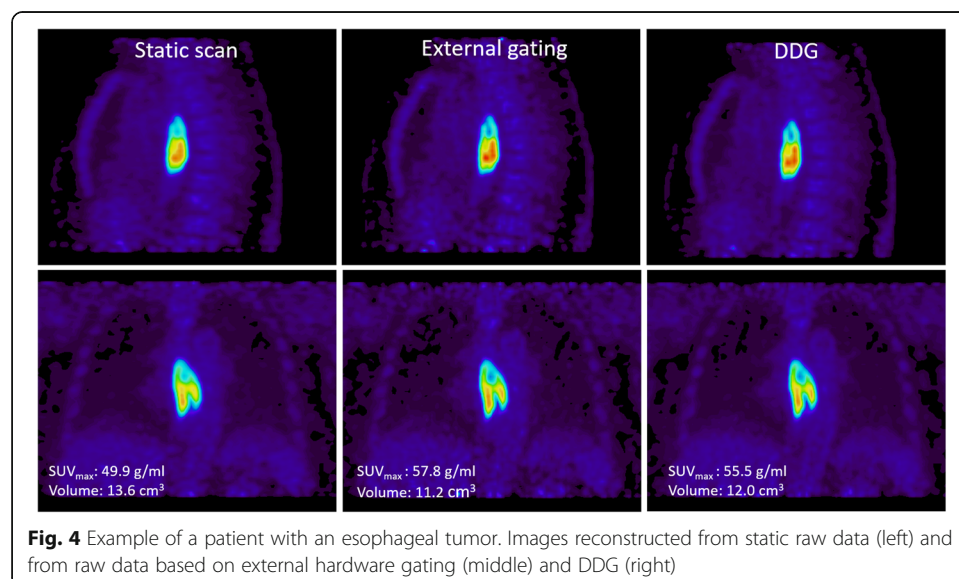


Table 1 Quantitative measures in a liver sphere with a diameter of 3 cm. Data represents mean value and range (* indicates significantly different value, $p < 0.01$, for DDG compared with either static or external device-gated acquisitions)

Measure	Static acquisition		Gated acquisition	
	First 0–3 min	Last 4–6 min	External device	DDG
SUV _{mean}	2.37 (1.59–2.73)	2.31 (1.62–2.67)	2.27 (1.54–2.65)	2.27 (1.56–2.63)
SUV _{SD}	0.53 (0.37–0.83)	0.52 (0.37–0.74)	0.53 (0.35–0.76)	0.37 (0.26–0.61)*
Noise level	0.225 (0.15–0.33)	0.223 (0.15–0.29)	0.235 (0.15–0.32)	0.165 (0.12–0.21)*
SNR	4.61 (3.07–6.51)	4.73 (3.05–6.45)	4.46 (2.96–6.46)	6.32 (4.67–8.50)*

noise level in images based on data-driven gating was significantly lower (noise level 0.165) than in images based on either external hardware gating (noise level 0.235) or regular static acquisition (noise level 0.223 and 0.225). Reduced noise level implies higher signal-to-noise values (Table 1) and thus improved image quality for the DDG images in this study, which is also visible in Fig. 4. This result is in contradiction with Walker et al. (Walker et al. 2020) who however only visually investigated the noise level in the liver and bone marrow in PET/CT data and found almost equivalent noise levels in images based on DDG, external hardware gating, and a static image from 50% of the coincidence data. In another study, evaluating respiratory gating based on signals extracted from PET raw data using PCA, the results showed significantly lower noise levels in images based on respiratory gating signals extracted from PET raw data using PCA compared with gated images based on respiratory gating signals extracted from external bellow device (Fürst et al. 2015).

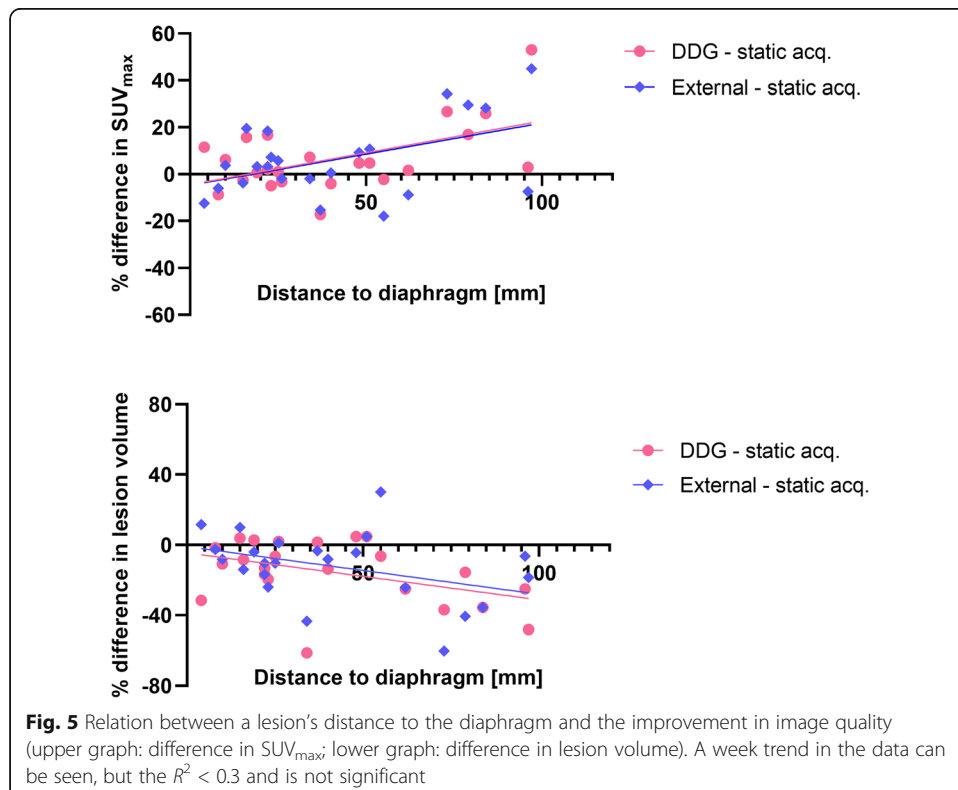
In order to evaluate and put the image quality improvement that respiratory gating achieves, in relation to the normal variation in image quality of two static acquisitions, we performed a test-retest study of the whole 6-min scan as two 3-min static acquisitions, the first 3 min and the last 3 min of acquisition. Interestingly, the paired *t*-test demonstrated a significant difference in SUV_{max} between the two static acquisitions. But still, both demonstrated lower average SUV_{max} than the DDG and external

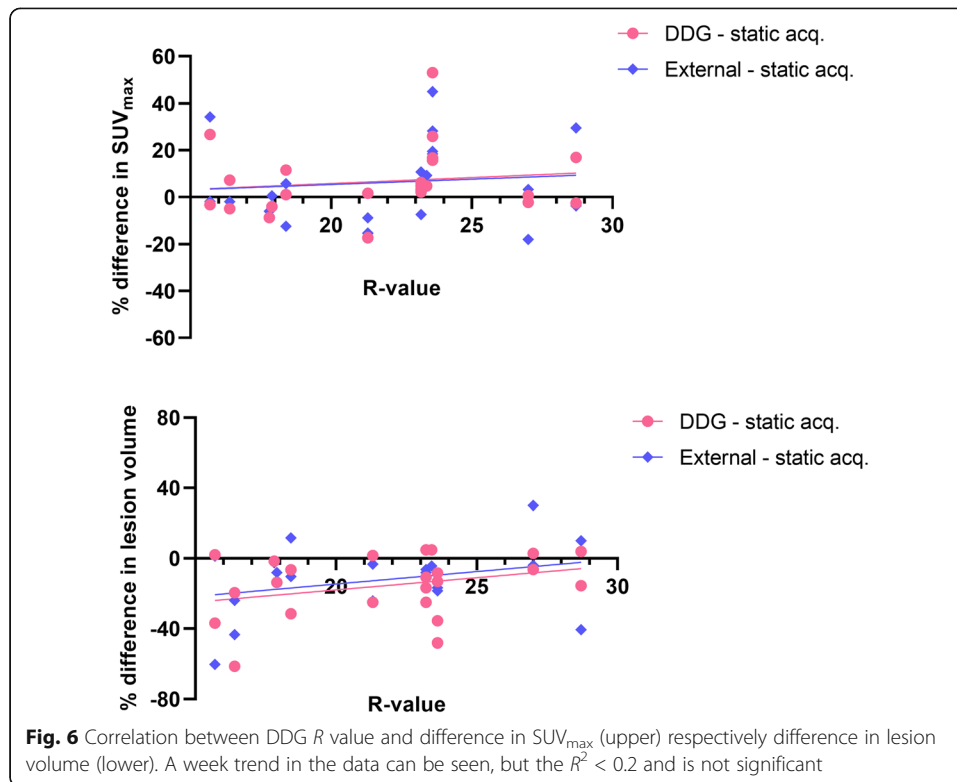


hardware gating provide. No significant difference in lesion volume was found between the two static acquisitions. Furthermore, the increase in SUV_{max} and decrease in lesion volume that breathing gating produces (see Fig. 3) appear to be large in relation to the scan-rescan variation of two static acquisitions.

The range of SUV_{max} values presented in this study was larger for the gating methods, both DDG and external hardware gating, than for the static acquisitions. The results demonstrated that breathing gating had larger impact on some patients or lesions than on other, but the increase in SUV did not have a strong correlation with an increased R -value or the lesion's distance to the diaphragm, see Figs. 5 and 6. Overall, the agreement in SUV_{max} between DDG and external device gating was very good in this study. In small lesions, $< 1 \text{ cm}^3$, the uncertainty in quantitative measurements becomes larger, and it is thus also in these lesions that we found the largest discrepancies between the gating methods (illustrated in Figs. 1 and 2).

We hypothesized that the impact from breathing gating methods would be larger in lesions located close to the diaphragm than more peripheral, but the results did not show any correlation between the lesion's distance to the diaphragm and increase in SUV_{max} , either between DDG and static acquisition or between external gating and static acquisition. In other studies, it seems like this parameter is of importance, at least when determining the R value or the impact of breathing motion in relation to location of the bed position, where PET beds located close to the diaphragm suffered from larger impact of motion (Beyer et al. 2003). In this study, a single bed position is included, and our results suggests that the location within that bed position is not relevant for the effect of breathing gating.





The present study shows a similar performance of DDG and external device gating in patients with esophageal tumors in a PET/MRI scanner. However, data-driven gating has some additional benefits compared to external device gating. First, and most important, it can be applied without need for any extra external device, which is time saving during the scanning procedure. Second, DDG resulted in reduced image noise compared to external device gating and static images. Third, it removes the risk of a possible time-synchronization error that can be introduced if the timing between the external device and the scanner is badly calibrated. Fourth, DDG can be used retrospectively in patients where image blurring has occurred due to extensive respiratory motion, but in that case at the expense of losing approximately 50% of the coincidence data.

Limitations

The results and analysis in this study are focused on quantitative measures, such as SUV_{max} , lesion volumes, and noise. Images have been visually assessed with respect to detect image artifacts and reconstruction errors, but the study does not include any thorough visual evaluation by an experienced observer. The relatively small number of patients and lesions is a limitation of this study, but despite this, clearly significant results were found.

Conclusion

Data-driven gating with MotionFree for PET-MRI performs similar to external device gating for esophageal lesions. Both gating methods significantly increased the SUV_{max} and reduced the lesion volume in comparison with non-gated static acquisition. DDG resulted in reduced image noise compared to external device gating and static images.

Abbreviations

DDG: Data-driven gating; FOV: Field of view; GEJ: Gastroesophageal junction; MRI: Magnetic resonance imaging; PET: Positron emission tomography; PCA: Principal component analysis; SNR: Signal-to-noise ratio; SUV: Standardized uptake value

Acknowledgements

We thank the patients who voluntarily joined this study. The authors also acknowledge the help from Anders Lundberg, Marie Åhlman, and Gunilla Andersson at the PET/MR-unit for scanning the patients and from research nurse Lena Ekfjord for coordinating the investigations with their cancer care.

Authors' contributions

SK contributed to the study design, performed the image reconstruction and the image analysis, performed the statistical analysis, and drafted the manuscript. NKH contributed in the data analysis and to the study design. EL and JS contributed in the data analysis. GL and JH contributed to the concept of the study and the patient recruitment. HA, TB, and ML contributed to the study design and the interpretation of data. All authors have revised the manuscript and approved the final version.

Funding

The study was supported by grants from the Bengt Ihre research Fund (JH), The Swedish Medical Association (JH), and Lennanders research Fund (GL). Swedish Cancer Society (CAN 2017/674 and CAN 2017/1086 (JH), Lion's Cancer fund (JH), and the Swedish Research council (number 822-2011-6269). ML and HA have received research support and speaker fees from GE Healthcare. Open Access funding provided by Uppsala University.

Availability of data and materials

The datasets used and/or analyzed during the current study are available from the corresponding author on reasonable request.

Declarations

Ethics approval and consent to participate

All patients provided written informed consent to participate in the study, and approval was granted from the regional medical ethics committee in Uppsala (DNR 2014/551).

Consent for publication

Not applicable.

Competing interests

The authors declare that they have no competing interests.

Author details

¹Radiology & Nuclear Medicine, Department of Surgical Sciences, Uppsala University, Uppsala, Sweden. ²Medical Physics, Uppsala University Hospital, Entrance 85, SE-751 85 Uppsala, Sweden. ³Medical Imaging Centre, Uppsala University Hospital, Entrance 85, SE-751 85 Uppsala, Sweden. ⁴Section of Gastrointestinal Surgery, Department of Surgical Sciences, Uppsala University, Uppsala, Sweden. ⁵Antaros Medical AB, Mölndal, Sweden.

Received: 18 December 2020 Accepted: 7 March 2021

Published online: 23 March 2021

References

- Bertolli O, Sanderson T, Alnaim A, Wan MYS, Wollenweber S, Stearns C et al (2018) Evaluation of data-driven respiratory gating in PET with PCA. *J Nucl Med* 59(supplement 1):9
- Beyer T, Antoch G, Blodgett T, Freudenberg LF, Akhurst T, Mueller S (2003) Dual-modality PET/CT imaging: the effect of respiratory motion on combined image quality in clinical oncology. *Eur J Nucl Med Mol Imaging* 30(4):588–596. <https://doi.org/10.1007/s00259-002-1097-6>
- Boellaard R, Delgado-Bolton R, Oyen WJG, Giammarile F, Tatsch K, Eschner W et al (2015) FDG PET/CT: EANM procedure guidelines for tumour imaging: version 2.0. *Eur J Nucl Med Mol Imaging* 42(2):328–354
- Büther F, Jones J, Seifert R, Stegger L, Schleyer P, Schäfers M (2020) Clinical evaluation of a data-driven respiratory gating algorithm for whole-body positron emission tomography with continuous bed motion. *J Nucl Med* 61(10):1520–1527
- Büther F, Vehren T, Schäfers KP, Schäfers M (2016) Impact of data-driven respiratory gating in clinical PET. *Radiology* 281(1):229–238. <https://doi.org/10.1148/radiol.2016152067>
- Fürst S, Grimm R, Hong I, Souvatzoglou M, Casey ME, Schwaiger M et al (2015) Motion correction strategies for integrated PET/MR. *J Nucl Med* 56(2):261–269. <https://doi.org/10.2967/jnumed.114.146787>
- Grimm R, Fürst S, Souvatzoglou M, Forman C, Hutter J, Dregely I, Ziegler SI, Kiefer B, Hornegger J, Block KT, Nekolla SG (2015) Self-gated MRI motion modeling for respiratory motion compensation in integrated PET/MRI. *Med Image Anal*. 19(1):110–120. <https://doi.org/10.1016/j.media.2014.08.003>
- Guérin B, Cho S, Chun SY, Zhu X, Alpert NM, El Fakhri G et al (2011) Nonrigid PET motion compensation in the lower abdomen using simultaneous tagged-MRI and PET imaging. *Med Phys* 38(6Part1):3025–3038
- Linder G, Korsavidou-Hult N, Bjerner T, Ahlström H, Hedberg J (2019) 18F-FDG-PET/MRI in preoperative staging of oesophageal and gastroesophageal junctional cancer. *Clin Radiol* 74(9):718–725. <https://doi.org/10.1016/j.crad.2019.05.016>
- Liu C, Pierce LA 2nd, Alessio AM, Kinahan PE (2009) The impact of respiratory motion on tumor quantification and delineation in static PET/CT imaging. *Phys Med Biol* 54(24):7345–7362

- Manber R, Thielemans K, Hutton BF, Barnes A, Ourselin S, Arridge S, O'Meara C, Wan S, Atkinson D (2015) Practical PET respiratory motion correction in clinical PET/MR. *J Nucl Med* 56(6):890–896. <https://doi.org/10.2967/jnumed.114.151779>
- Soussan M, Comtat C, Brulon V, Helal O, Buvat I. Dual-modality respiratory triggering is feasible during a routine PET/MR protocol. *J Nucl Med* 2016;57(supplement 2):242–242. [cited 2020 Oct 29]
- Thielemans K, Rathore S, Engbrant F, Razifar P (2011) Device-less gating for PET/CT using PCA. In: 2011 IEEE Nuclear Science Symposium Conference Record, pp 3904–3910
- Walker MD, Bradley KM, McGowan DR (2018) Evaluation of principal component analysis-based data-driven respiratory gating for positron emission tomography. *Br J Radiol* 91(1085):20170793
- Walker MD, Morgan AJ, Bradley KM, DR MG (2019) Evaluation of data-driven respiratory gating waveforms for clinical PET imaging. *EJNMMI Res* 9(1):1
- Walker MD, Morgan AJ, Bradley KM, McGowan DR (2020) Data driven respiratory gating outperforms device-based gating for clinical FDG PET/CT. *J Nucl Med*
- Würslin C, Schmidt H, Martirosian P, Brendle C, Boss A, Schwenzer NF et al (2013) Respiratory motion correction in oncologic PET using T1-weighted MR imaging on a simultaneous whole-body PET/MR system. *J Nucl Med* 54(3):464–471. <https://doi.org/10.2967/jnumed.112.105296>

Publisher's Note

Springer Nature remains neutral with regard to jurisdictional claims in published maps and institutional affiliations.

Submit your manuscript to a SpringerOpen[®] journal and benefit from:

- ▶ Convenient online submission
- ▶ Rigorous peer review
- ▶ Open access: articles freely available online
- ▶ High visibility within the field
- ▶ Retaining the copyright to your article

Submit your next manuscript at ▶ [springeropen.com](https://www.springeropen.com)
